Geophysical Journal International

Geophys. J. Int. (2012) **190,** 922–930 doi: 10.1111/j.1365-246X.2012.05531.x

High resolution dynamic ocean topography in the Southern Ocean from GOCE

A. Albertella,[1] R. Savcenko,[2] T. Janjić,[3] R. Rummel,[1] W. Bosch[2] and J. Schröter[3]

[1] *Institut für Astronomische und Physikalische Geodäsie, TU München, Arcistrasse* 21, 80290 *Munich, Germany. E-mail: albertella@bv.tum.de*
[2] *Deutsches Geodaetisches Forschungs Institut, Alfons-Goppel-Strasse* 11, 80539 *Munich, Germany*
[3] *Alfred Wegener Institute for Polar and Marine Research, Postfach* 120161, 27515 *Bremerhaven, Germany*

Accepted 2012 May 1. Received 2012 May 1; in original form 2011 February 21

SUMMARY

A mean dynamic ocean topography (MDT) has been computed using a high resolution GOCE (Gravity field and steady-state Ocean Circulation Explorer) gravity model and a new mean sea surface obtained from a combination of satellite altimetry covering the period 1992 October till 2010 April. The considered gravity model is GO-CONS-GCF-2-TIM-R3, which computes geoid using 12 months of GOCE gravity field data. The GOCE gravity data allow for more detailed and accurate estimates of MDT. This is illustrated in the Southern Ocean where the commission error is reduced from 20 to 5 cm compared to the MDT computed using the GRACE gravity field model ITG-Grace2010. As a result of the more detailed and accurate MDT, the calculation of geostrophic velocities from the MDT is now possible with higher accuracy and spatial resolution, and the error estimate is about 7 cm s^{-1} for the Southern Ocean.

Key words: Satellite gravity; Global change from geodesy; Antarctica.

1 INTRODUCTION

On 2009 March 17 the satellite GOCE (Gravity field and steady-state Ocean Circulation Explorer) was launched (ESA 1998, 2006). The mission objectives of GOCE are the determination of the global gravity field and geoid with high accuracy and spatial resolution. More specifically GOCE aims at a geoid accuracy of 1–2 cm with a spatial resolution of about 100 km, corresponding to a spherical harmonic expansion complete up to degree and order 200 (Rummel *et al.* 2002; Drinkwater *et al.* 2003). The core instrument of GOCE is a three axis gravitational gradiometer, the first of its kind in space. A rather complex sensor system had to be developed in order to ensure the high quality of the measured gradients. The mission characteristics are described in Rummel (2010) and in Rummel & Gruber (2010). Almost twelve months of mission data have been processed and the first preliminary spherical harmonic models constructed. In this study a pure satellite model derived from GOCE data is considered. It is the GO-CONS-GCF-2-TIM-R3 model (GOCE-TIM3 in the following), complete up to degree 250 and computed using the timewise approach (Pail *et al.* 2010).

The intention of this paper is to look into the use of a GOCE high resolution geoid model for the computation of mean dynamic ocean topography (MDT) and geostrophic velocities. The chosen area of investigation is the Southern Ocean. As reported by Griesel *et al.* (2012), topography is complex there, with rather short spatial scales and high temporal variability. Furthermore, at times large parts of the Southern Ocean are covered by sea ice affecting both satellite altimetry measurements as well as *in situ* oceanographic data available for an independent validation.

The principles of computation of geodetic mean topography were discussed by Hughes & Bingham (2008). They are primarily related to the consistency of the altimetric mean sea surface (MSS) and the geodetic surface in terms of coordinate system, reference ellipsoid and permanent tide system. The basic principles were also discussed in Bingham *et al.* (2008), and more recently, in Haines *et al.* (2011). In Bingham *et al.* (2008), the important issue of spectral consistency of the altimetric and geoid surface is addressed. The authors favour the so-called global approach, which represents the MDT as a spherical harmonic series. It was introduced by Tapley *et al.* (2003). This technique will also be followed here, because it permits to quantify the signal content in selected spectral windows. A problem of this approach is the need to complement the altimetric surface of the ocean by a corresponding surface on land, usually a high resolution so-called combined geoid model. Distortions in the spectral representation, in particular along the coastlines, cannot be avoided (Albertella & Rummel 2009). Spectral consistency of the altimetric sea surface and the geoid is attained by filtering. Challenges are the signal attenuation, distortions along coastlines, narrow topographic features and Gibbs oscillations (Bingham *et al.* 2008). Anisotropic filtering may serve as a remedy, as proposed in Bingham (2010) and in Bingham *et al.* (2011).

The high spectral resolution of GOCE helps to capture small scale features of MDT and of geostrophic velocities and to reduce the effects of filtering. First experiments with GOCE geoid models are the mean dynamic topography computations in the Arctic Ocean by Farrel *et al.* (2012), the North Atlantic study by Bingham *et al.* (2011) and the global as well as regional study by Knudsen *et al.* (2011). Here we look into the benefit of the high spatial resolution of

GOCE in the Southern Ocean studying mean dynamic topography and geostrophic velocities as well as the corresponding propagation of the error variance–covariance. The global approach in terms of spherical harmonic series will help with a quantification of the higher spatial resolution.

The characteristics of the new altimetric MSS as well as comparisons with alternative models are described in Section 2.1. In Section 2.2, a summary of the gravity field model GOCE-TIM3 is given. The key ocean quantity in our application is the MDT. It is derived from the height difference between the MSS and the geoid. Its derivation is discussed in Section 3. This section also includes a discussion of regional MDT models and an analysis of their spatial and spectral properties. In Section 4 geostrophic velocities as derived from the MDT are studied. In order to validate the results, a comparison with independent *in situ* measurements is presented in Section 5. Section 6 contains the conclusions.

2 DATA

2.1 MSS

Altimeter satellites provide precise, repeated, and quasi-global measurements of sea surface heights. A MSS is a temporal average of these sea surface heights over a chosen period of time. As the present investigation aims at the determination of a quasi-stationary MDT, the MSS should represent a reliable long-term mean.

A new MSS (DGFI10) has been generated, averaging the measurements of altimeter missions with exact repeat periods (ERS-1/2, ENVISAT, TOPEX/Poseidon, Jason-1 and Jason-2), acquired within the period from 1992 October to 2010 April. The period 1992–2010 exhibits a rather homogeneous data distribution and ensures that the MSS is hardly affected by seasonal variations or interannual variability like the 1997/1998 El Nino. The MSS heights are computed at the nodes of a regular $30' \times 30'$ geographical grid, corresponding to a grid spacing of 55 km, which is far below the smallest filter length of the low pass filter, applied to generate the MDT (see Section 3).

The DGFI10 MSS is constructed by a careful pre-processing of the altimeter measurements followed by a remove-gridding-restore method. The pre-processing includes:

(i) Application of the most recent orbits and mission specific correction models (e.g. for the sea state bias), see Chambers *et al.* (2003), Iijima *et al.* (1999), Scharroo & Smith (2010), Scharroo & Visser (1998) and Schrama *et al.* (2000).

(ii) Harmonization by applying identical geophysical reduction models as far as possible (e.g. for ocean tides), see Mayer-Gürr *et al.* (2011).

(iii) Cross-calibration to estimate radial errors and range biases for each of the altimeter missions (for details see Dettmering & Bosch 2010a,b).

The ultimate goal of the pre-processing is to generate homogeneous and consistent multimission data which can be readily merged for the MSS computation. The interpolation of the pre-processed altimeter data to the $30' \times 30'$ grid was performed with instantaneous sea surface heights reduced by a reference surface, here the CLS01 MSS (Hernandez & Schaeffer 2000). Compared to sea surface heights ($\approx \pm 100$ m), the instantaneous sea surface heights (<1 m) have significantly reduced gradients and are therefore much easier to interpolate. The along-track instantaneous heights were then averaged to fixed points along the nominal ground track and in a second step all mean instantaneous sea surface heights within the grid cells were averaged to a multimission mean anomaly. Finally, the CLS01 sea surface heights within the $30' \times 30'$ grid cells (themselves sampled with $2'$ spacing) were averaged and added back to the multimission mean anomaly. In this way the DGFI10 MSS represents a MSS for the period 1992–2010 with heights (averaged over $30' \times 30'$) defined on the nodes of a $30' \times 30'$ grid.

Table 1. Statistics (in centimetres) of the differences between DGFI10 and CLS01, CLS10 and DTU10.

	Mean	rms	Min	Max
CLS01-DGFI10	−1.13	2.37	−29.86	21.86
CLS10-DGFI10	−0.72	2.21	−31.62	25.79
DTU10-DGFI10	2.28	3.04	−23.47	27.81
CLS10-CLS01	0.41	1.27	−30.95	25.98
DTU10-CLS01	3.41	4.27	−23.98	36.55
DTU10-CLS10	3.00	3.90	−14.06	45.21

In order to validate the DGFI10 MSS, a comparison with other MSS models recently published was performed. Besides CLS01 (Hernandez & Schaeffer 2000), the updated MSS CLS10, produced in 2010 by CLS Space Oceanographic Division and distributed by AVISO with support from CNES (http://www.aviso.oceanobs.com) is considered. Furthermore DGFI10 is compared with the DTU10 MSS, an update of DNSC08 (Andersen & Knudsen 2009). These external MSSs are based on different sets of altimeter missions; they are related to other averaging periods and differ in the treatment of the inverted barometer effect. Over land areas all these external MSSs are augmented by geoid heights with a smooth transition between geoid and sea surface heights at coastal zones. A detailed description of the individual processing schemes is outside of scope of this paper.

Important for the comparison is the fact that the external MSSs are provided with a high spatial resolution of $2' \times 2'$ (CLS and CLS10) or even $1' \times 1'$ (DTU10). Consequently these MSS have to be pre-processed in order to achieve the same resolution as DGFI10 MSS for the comparison. This was done by averaging of all sea surface heights within $30' \times 30'$ grid cells to ensure the spectral consistency to the DGFI10 MSS. The comparison was then performed for grid nodes in open ocean, excluding a coastal zone of 100 km to prevent that the statistics, summarized in Table 1, being dominated by systematic effects at the coast. The global rms values are surprisingly small and remain below 5 cm. The best agreement is between CLS01 and CLS10 which use the same averaging period (1993–1999). The rms differences of DGFI10 MSS to the others are below 3.04 cm. The advantage of our computation of an MSS is the full control over all processing steps and the use of the most recent standards, reductions and orbit.

2.2 Geoid

The satellite gravity field GOCE-TIM3 is a GOCE-only solution based on measurements from 2009 November to 2011 April of GOCE orbits and gravity gradients. It is a GOCE-only result in a strict sense, that is, no prior gravity field information entered the computation. It is computed using the timewise approach, see Pail *et al.* (2010) and Pail *et al.* (2011), and it is available up degree/order 250. In Fig. 1 the cumulative geoid error of GOCE-TIM3 is compared with that of the pure GRACE solution ITG-Grace2010 (Mayer-Gürr *et al.* 2010). In the low degrees the low-low

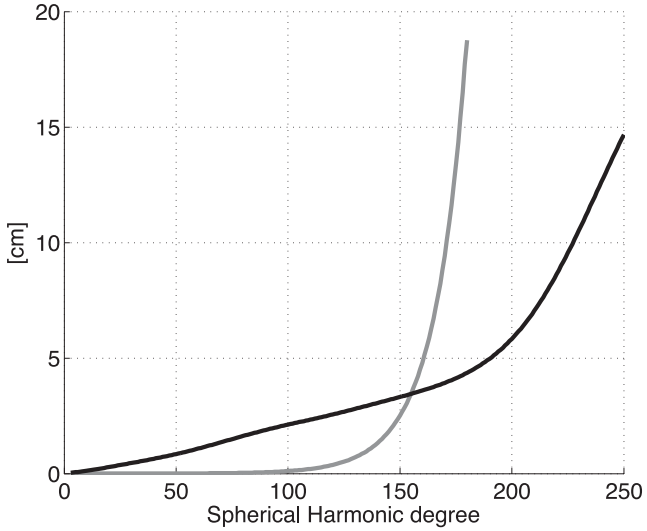

Figure 1. Cumulative geoid errors (in centimetres) for the GRACE satellite-only model ITG-Grace2010 (grey line), the GOCE satellite-only model GOCE-TIM3 (black line).

Satellite-to-Satellite Tracking (SST) concept of GRACE is superior to GOCE, the latter starts to become superior starting from degree 155. At degree $L = 200$ the cumulative geoid error of GOCE-TIM3 is around 6 cm, still higher than the projected 2 cm. The accumulation of more data is expected to improve the quality of the model.

3 MEAN DYNAMIC OCEAN TOPOGRAPHY

The MSS is expressed as height h above a chosen reference ellipsoid. Likewise the geoid surface—which represents the ocean surface at rest—is given in terms of geoid heights N above a chosen reference ellipsoid. The difference between the MSS height h and the geoid height gives the steady-state MDT, H, that is,

$$H = h - N. \tag{1}$$

In order to compute a consistent geodetic MDT, first of all, some indispensable corrections must be applied to the data, (Hughes & Bingham 2008). Geoid and MSS must refer to a common reference system, as described, for example, in Heiskanen & Moritz (1967): the geoids GOCE-TIM3 and ITG-Grace2010 are referred to the GRS80 ellipsoid, while the MSS referred to the Topex/Poseidon ellipsoid.

Geoid and MSS must also be defined in the same permanent tide system. The ITG-Grace2010 model refers to zero tide system (the permanent direct effects of the Sun and Moon are removed, but the indirect effect related to the elastic deformation of the Earth is retained) while the GOCE-TIM3 refers to tide free system where all effects of Sun and Moon are removed applying conventional Love numbers. The latter are not measurable and are therefore theoretical to some extent. The MSS is usually defined in the mean tide system (no permanent tide effects are removed). The transformation between the different tide systems can be applied directly to the spherical harmonic coefficients (Smith 1998) or by adding the tide correction to the geoid heights (Rapp 1989). The geoid is here referred to the Topex/Poseidon ellipsoid and defined in the mean tide system.

Finally geoid and MSS must be expressed using the same coordinate system; here ellipsoidal coordinates are considered.

A more critical point are the different spectral characteristics of h and N, (Bingham *et al.* 2008). The geoid is defined globally over the whole surface of the earth. Its resolution is expressed by the maximum degree of its spherical harmonic representation

$$N(\vartheta_P, \lambda_P) = R \sum_{\ell=2}^{L} \sum_{m=0}^{\ell} (C_{\ell m} \cos m\lambda_P + S_{\ell m} \sin m\lambda_P)\, P_{\ell m}(\cos \vartheta_P). \tag{2}$$

Here, R is the mean earth radius, (ϑ_P, λ_P) are the spherical co-latitude and longitude of the point P, $C_{\ell m}$ and $S_{\ell m}$ are the normalized, non-dimensional, spherical harmonic coefficients, L is the highest degree considered in the spherical harmonic expansion, $P_{\ell m}$ are the fully normalized associated Legendre functions of degree ℓ and order m.

For all degrees (and orders) less than or equal to L, the coefficients of the geoid and their error variances (the commission error) are available. The signal for degrees above L is the omitted signal or omission error. The degree L corresponds approximately to a spatial scale of $20\,000/L$ km, consequently the gridded geoid field does not contain spatial scales less than this.

The MSS data represent local sea level averaged and interpolated onto nodes of the regular $30' \times 30'$ grid (about 55 km $\times$ 55 km at the equator). The original data are altimetric measurements densely available along satellite tracks; these measurements contain information with high spatial resolution. The short scale altimetric features will contain both dynamic topography and geoid features not contained in eq. (2) that must be removed by filtering, to make sure that the computed MDT is consistent with the spatial resolution of the geoid field, (Bingham 2010). Furthermore Losch *et al.* (2002) show that geoid and MSS should have the same representation using same base functions. Otherwise the omission error may leak in the commission error.

In this paper h and N are combined in terms of spherical harmonics, similar to Bingham *et al.* (2008). This requires extension of the altimetric MSS over land areas. In our case the MSS is complemented on land by geoid heights, computed from the EGM08 gravity model up degree and order 180

$$h^{\text{ext}} = \begin{cases} h & \text{on ocean} \\ N_{EGM08} & \text{on land} \end{cases} \tag{3}$$

allowing its representation in terms of spherical harmonic series. The distortions along the transition zone from ocean to land cannot be completely eliminated (Albertella & Rummel 2009), but they can be strongly reduced by iteratively applying a sequence of spherical harmonic analysis and synthesis (Albertella *et al.* 2010), or, as done here, by using a moving window operator. In the latter case, the value in each point on the land areas is replaced by an average of the adjacent values by

$$\bar{h}^{\text{ext}}(\vartheta_i, \lambda_j) = \frac{1}{(2k+1)^2} \sum_{k} h^{\text{ext}}(\vartheta_{i+p}, \lambda_{j+q}) \tag{4}$$

with $p = -k, \ldots, k$ $q = -k, \ldots, k$. Depending on the position of each point (ϑ_i, λ_j) relatively to the land–ocean transition, both values, MSS and geoid height, will contribute to $\bar{h}^{\text{ext}}$. The procedure of spherical harmonic expansion is repeated several times maintaining in each step the original values at sea and considering the new set of mean values on land. Thirty iterations, with $k = 4$, are sufficient to remove significant variations along the coastlines.

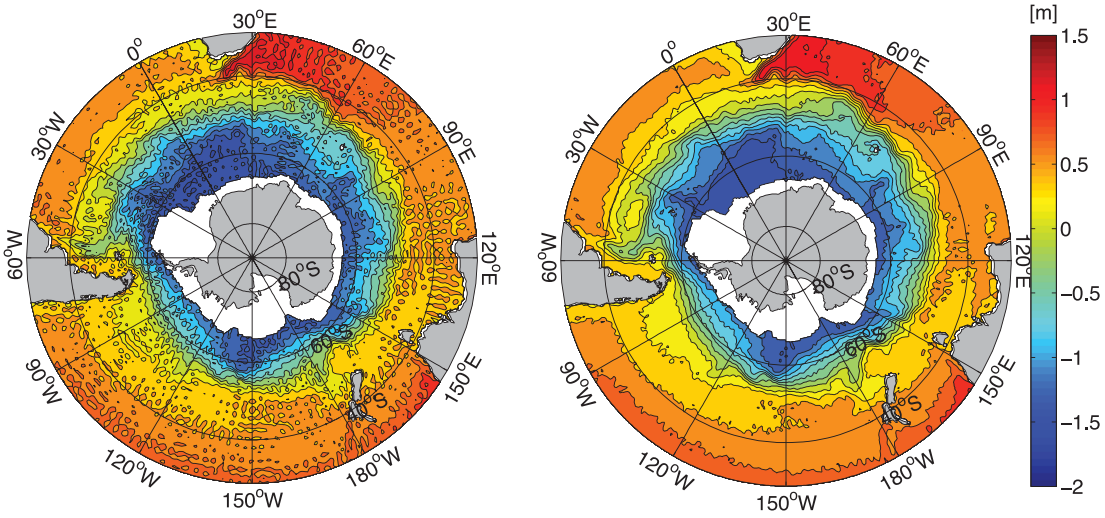

Figure 2. MDT in the ACC area. Gauss filter corresponding to degree 180 is applied. Gravity model ITG-Grace2010 (left-hand panel) and GOCE-TIM3 (right-hand panel) gravity models are considered. Units are metres.

The spectral consistency is achieved by applying the same Gauss-type filter to MSS and to the geoid. The Gauss filter exhibits no side lobes in the spectral as well in the spatial domain, see Jekeli (1981) and Wahr *et al.* (1998). It corresponds to a weighted moving averaging with a defined spherical radius r in the space domain. As described in Zenner (2006), the half-weight radius r of the filter is related to the harmonic degree L of the spectrum by the empirical relation

$$r \approx \frac{1.45 \times 10^4}{L} \,. \tag{5}$$

Unfortunately the shape of the filter in the spectral domain causes that some short scale dynamic topography signal is removed too, by filtering (Bingham *et al.* 2008).

In Fig. 2 the MDT computed using the gravity model ITG-Grace2010 (left-hand panel) is compared with the MDT computed using GOCE-TIM3 gravity model (right-hand panel). The filtering, here up degree $L = 180$, is not able to eliminate the short scale distortions in the GRACE solution and the oceanic signal is partially obscured. The MDT from GOCE data shows more oceanographic details, reflecting the features related to the major ocean currents. At these scales (≈111 km) the complexity of the ocean topography becomes clearly visible; more details appear e.g. in the area of the Drake Passage and of the Aghulas current. Furthermore it is possible to observe detailed structures along the Antarctic Circumpolar Current (ACC).

The MDT is now globally defined and it is represented as series of spherical harmonic functions (Bingham *et al.* 2008):

$$H(\vartheta_P, \lambda_P) = R \sum_{\ell=0}^{L} \sum_{m=0}^{\ell} \left(C^H_{\ell m} \cos m\lambda_P + S^H_{\ell m} \sin m\lambda_P \right) P_{\ell m}(\cos \vartheta_P) \tag{6}$$

with the coefficients $C^H_{\ell m}$, $S^H_{\ell m}$ being the difference between the filtered coefficients of the SH-expansion of the MSS and $C_{\ell m}$, $S_{\ell m}$ of eq. (2).

Based on eq. (6) it is possible to analyze the spectral content of the MDTs in various bandwidths, giving insight into where the characteristics of GRACE and GOCE data are distinguishable. Strictly speaking the spherical harmonic representation of the MDT, eq. (6), can only be divided into spectral bands, if they are independent, that is, if there exist no correlations between the coefficients of the various bands. In reality some (rather small) correlations exist. Neglecting them here has only a small effect.

In Fig. 3, different bandwidths of the MDT computed using the gravity model ITG-Grace2010 (upper panel) are compared with the corresponding bandwidths of the MDT computed using GOCE-TIM3 (lower panel) in the area of the ACC. In the first band, from spherical harmonic degree 90 up 120 (first column), the spectral content is almost the same. Already between 120 and 150 (second column) the MDT band based on GRACE is significantly noisier, while typical ocean current features are still clearly discernible up to degree 180 when GOCE-TIM3 model is used. This demonstrates that (i) such short scales still contain significant oceanographic signal and (ii) that this signal can be discerned using a GOCE high resolution gravity model.

The error variance–covariance matrix C_{HH} of H, from eq. (1), is

$$C_{HH} = C_{hh} + C_{NN} - 2C_{hN} \,. \tag{7}$$

Here C_{hh} is the variance–covariance matrix of the MSS, C_{NN} the variance–covariance matrix of the geoid heights and C_{hN} the covariances between h and N. In first approximation the covariances of h can be neglected and its variances can be considered to be constant σ_h^2. In a second approximation we confine the C_{NN} matrix to its diagonal part, that is, to the error variances, neglecting the correlations between the spherical harmonic coefficients of the gravity model, see also van van Gelderen & Koop (1996). Furthermore the correlations between N and h are assumed to be zero, recalling that N and h are derived from independent measurements. After these simplifications we arrive at

$$\mathrm{diag}(C_{HH}) = \sigma_h^2 \cdot \mathrm{diag}(I) + \mathrm{diag}(C_{NN}) \,. \tag{8}$$

From the harmonic coefficient error variances, provided together with each of the gravity models, it is possible to propagate the error to the MDT. Here σ_h^2 is taken 9 cm^2. As shown in Fig. 4, the total error rms of the GRACE MDT is around 20 cm, while the error rms of the MDT using GOCE-TIM3 is about 5 cm. In both cases the total error is slightly varying with latitude. The improvement of the larger set of the GOCE data is visible in the band from d/o 150–180. The MDT's errors confirm that, while the MDT from GRACE data is accurate on long spatial scales, the use of GOCE information is necessary to describe correctly the shorter scales.

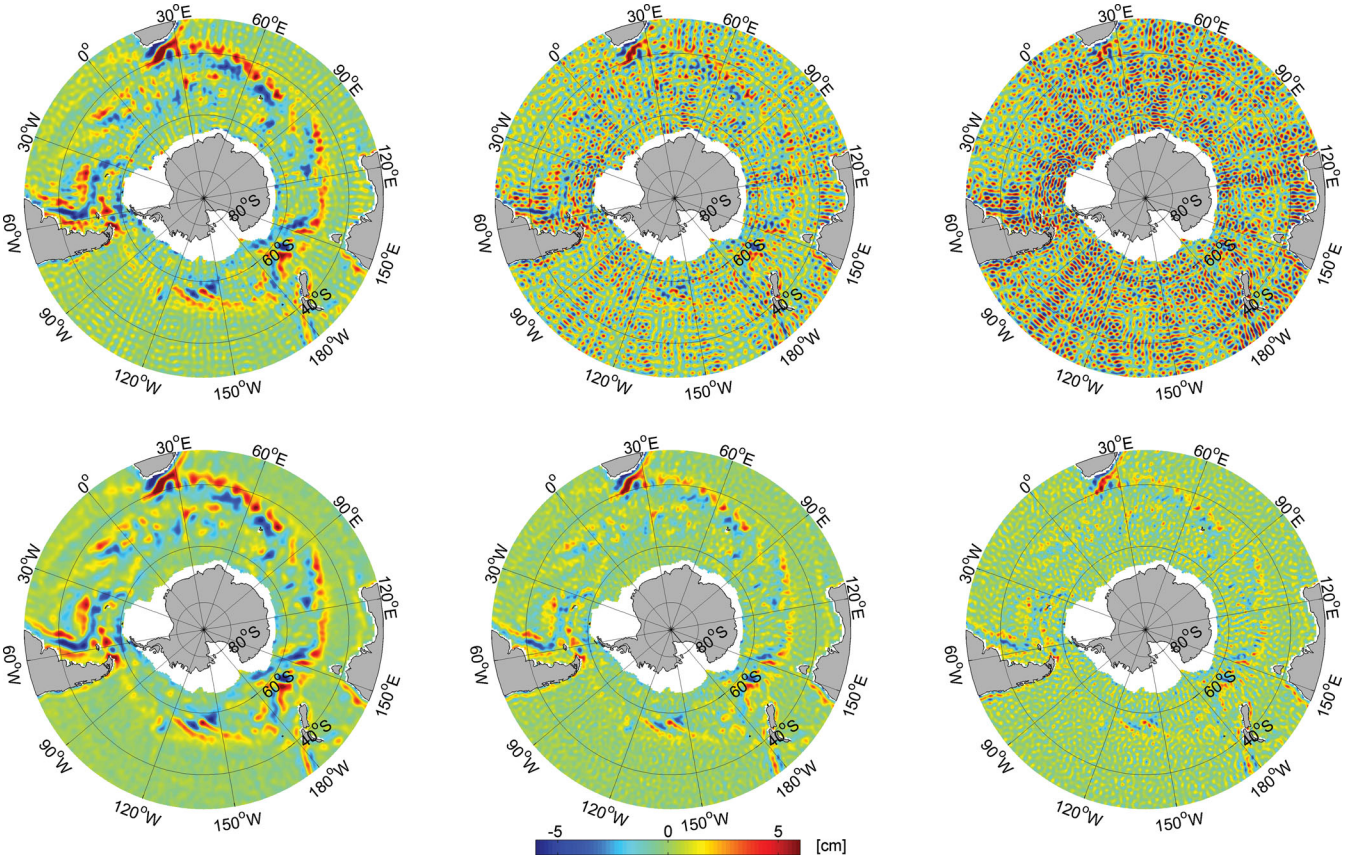

Figure 3. MDT in different bandwidths computed using ITG-Grace2010 (upper panel) and GOCE-TIM3 (lower panel). The harmonic components from 90 to 120 (left-hand panel), from 120 to 150 (middle panel) and from 150 to 180 (right-hand panel) are shown. Units are centimetres.

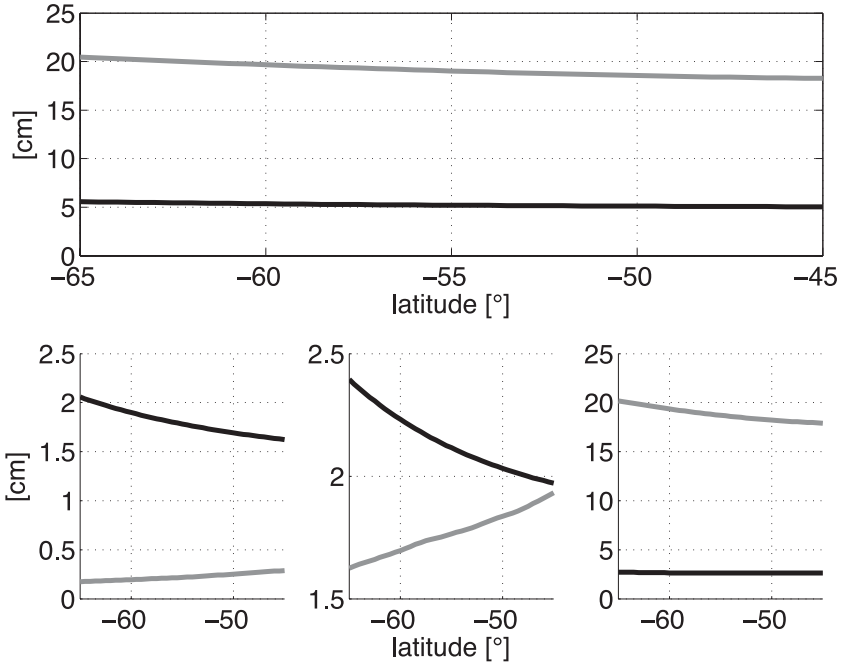

Figure 4. Comparison between the propagated errors from the harmonic coefficients to MDT in the area of the ACC area as function of latitude. Two gravity models are considered: ITG-Grace2010 (grey line) and GOCE-TIM3 (black line). The error of the MSS is considered uncorrelated with an rms value equal to 3 cm. The upper panel shows the cumulative error up degree $L = 180$. In the lower panel the MDT errors in different bands are shown considering the harmonic components from 90 to 120 (left-hand panel), from 120 to 150 (middle) and from 150 to 180 (right-hand panel). Units are centimetres.

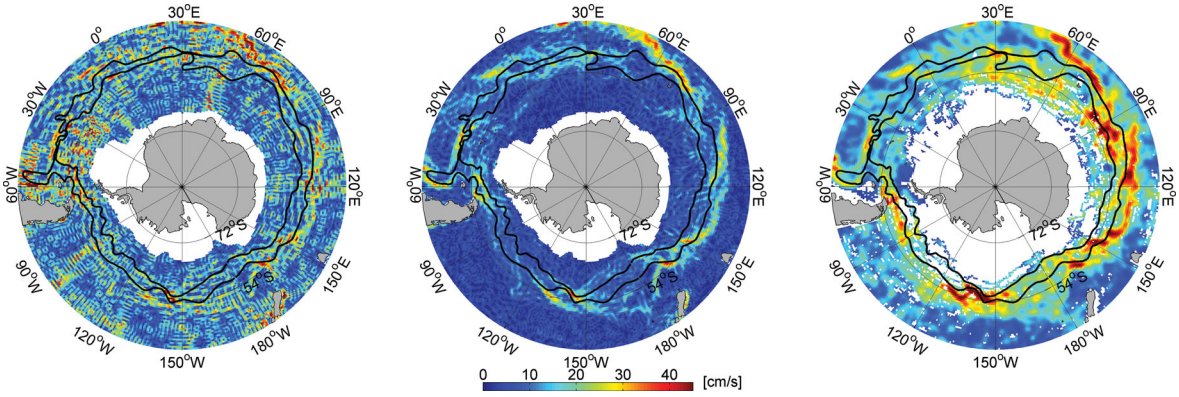

Figure 5. Magnitude of the geostrophic velocities in the ACC region. The geostrophic velocities, computed from the MDT relative to ITG-Grace2010 (left) and to GOCE-TIM3 (middle), are Gauss filtered corresponding to degree $L = 180$. The black lines are the fronts of the ACC computed from *in situ* measurements. In the right panel the geostrophic velocities from *in situ* measurements and corrected as described in Section 5 are shown. Areas without measurements are indicated with white color. Units are cm s^{-1}.

4 GEOSTROPHIC VELOCITIES

The gradient of the MDT is directly related to the geostrophic currents. The formulas for the surface geostrophic velocities of the ocean circulation, in longitude (east) and in latitude (north) direction are:

$$u_s = -\frac{g}{f}\frac{1}{R}\frac{\partial H}{\partial \vartheta}$$
$$v_s = \frac{g}{f}\frac{1}{R\sin\vartheta}\frac{\partial H}{\partial \lambda}. \tag{9}$$

Here g is the gravitational acceleration, $f = 2\Omega\cos\vartheta$ the Coriolis term and Ω the angular velocity of the earth. With the MDT expressed in a series of spherical harmonic functions, eq. (6), the surface velocities as function of the harmonic coefficients $C^H_{\ell m}$, $S^H_{\ell m}$ become:

$$u_s(\vartheta_P, \lambda_P) = -\frac{g}{f}\frac{1}{R}\sum_{\ell=0}^{L}\sum_{m=0}^{\ell}\left(C^H_{\ell m}\cos m\lambda_P + S^H_{\ell m}\sin m\lambda_P\right)P'_{\ell m}(\cos\vartheta_P) \tag{10}$$

$$v_s(\vartheta_P, \lambda_P) = \frac{g}{f}\frac{1}{R\sin\vartheta_P}\sum_{\ell=0}^{L}\sum_{m=0}^{\ell} m\left(-C^H_{\ell m}\sin m\lambda_P + S^H_{\ell m}\cos m\lambda_P\right)P_{\ell m}(\cos\vartheta_P), \tag{11}$$

where $P'_{\ell m}$ is the first derivative with respect to ϑ of the associated Legendre function $P_{\ell m}$. The direction (azimuth) of the resulting surface current vectors is $A = \arctan\left(\frac{u_s}{v_s}\right)$ and their length is $V = \sqrt{u_s^2 + v_s^2}$, (Elema 1993).

The use of the spherical harmonic coefficients to derive the geostrophic velocities allows (i) to avoid approximations inherent in numerical differentiation based on grid values of the MDT and (ii) the analysis of spectral bands. Since the step from MDT to surface velocities involves the surface gradient field, high degrees and orders of the spherical harmonic expansion get amplified. This is the same as saying, short scales features are emphasized. Consequently the strength of GOCE at shorter scales should become more pronounced, when comparing velocities.

In Fig. 5 the magnitudes of the geostrophic velocities in the ACC area are shown. The velocities computed using ITG-Grace2010 (left-hand panel) and GOCE-TIM3 (middle panel) are compared with the geostrophic velocities derived, as described below, from *in situ* measurements (right-hand panel). Superimposed on the figures are the locations of the Subantarctic and Polar fronts as estimated from historical data (Orsi *et al.* 1995). These two major fronts are continuous features of the ACC. Stronger velocities are observed in the areas where these fronts are quite close to one another and where the current meanders. The location of 40S between 40E to 80E marks the area where the Subantarctic and Subtropical front are close, again resulting in higher velocities. The results from GRACE data show the ringing also seen in the MDT, while the information from GOCE displays all the stronger currents in this area, following what the *in situ* measurements show.

The analysis of the spectral content of the geostrophic velocities in different bandwidths, Fig. 6, shows the noise behaviour in the chosen spectral bands. Noisy information is already present between 90 and 120 if only GRACE data are used for the geoid (upper panel). The velocities derived from GOCE-TIM3 (lower panel) are less noisy, though between 150 and 180 the signal is partially affected by noise. Nevertheless the Aghulas current and the East Australian current are still clearly visible.

The accuracy of the velocity fields depends on the accuracy of the spherical coefficients of the MDT. From formulas (10) and (11) the errors of the geostrophic surface velocity field can be calculated, also considering different bandwidths. The total error obtained considering ITG-Grace2010 is around 40 cm s^{-1}, while the rms error of the surface velocities using GOCE-TIM3 is about 10 cm s^{-1}, at all latitudes, see Fig. 7. Thus, as expected, in the case of the surface geostrophic velocities the refinement coming from GOCE, in particular in the bandwidth from 150 to 180, is significant. Compared with the rms of the geostrophic velocities in the ACC area, 10 cm s^{-1} is not negligible, however. When the mission GOCE will be concluded and all its measurements will be available, a further improvement of this value can be expected.

5 VALIDATION OF THE RESULTS

The geostrophic velocities, as computed from the geodetic MDT, are validated by comparison with independent *in situ* measurements. The Global Drifter Program of NOAA and AOML collected satellite-tracked drifting buoys (drifter in the following) measurements of upper ocean currents and sea surface temperatures

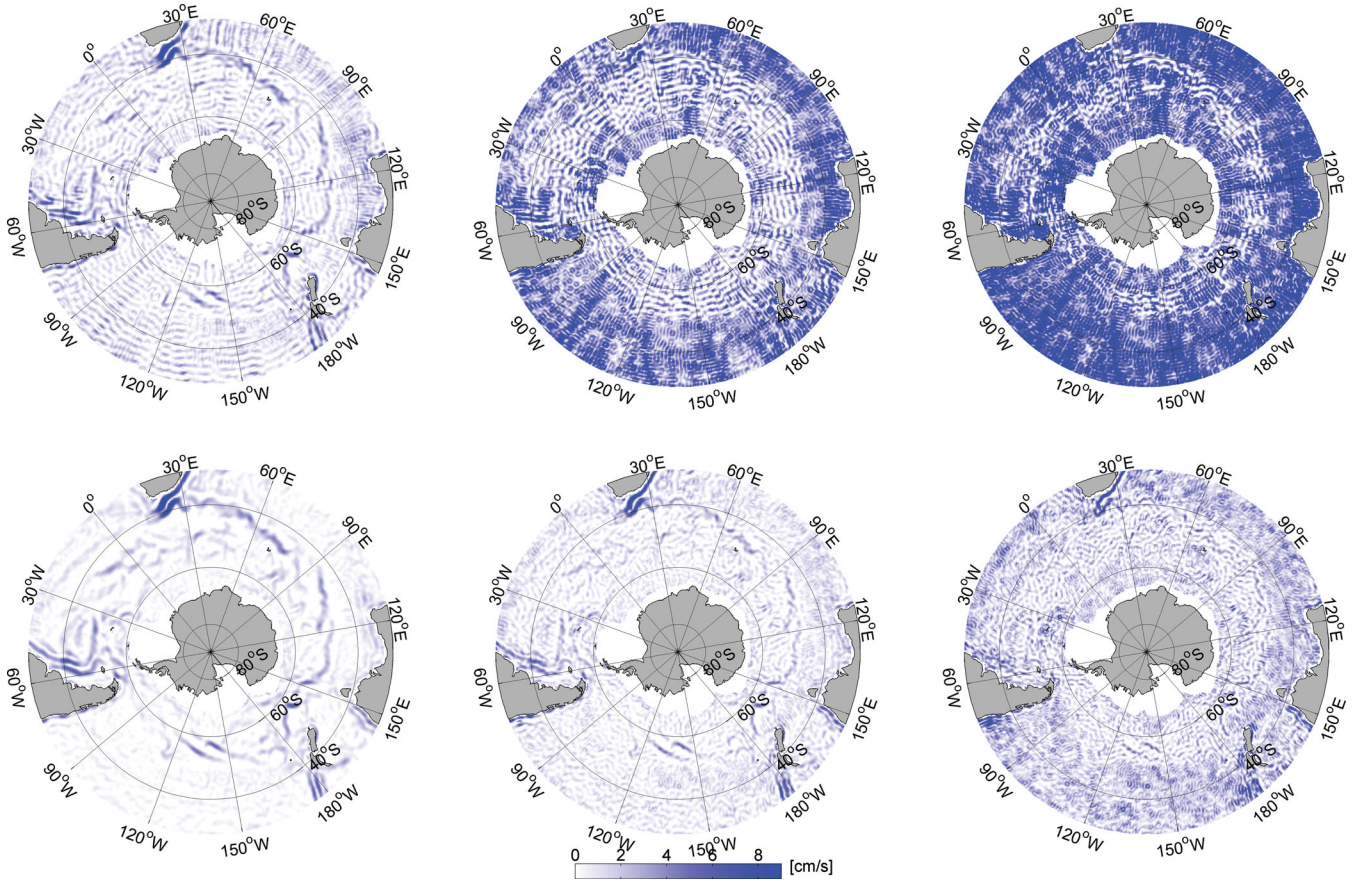

Figure 6. Magnitude of the geostrophic velocities in different spectral bands computed from MDT using ITG-Grace2010 (upper panel) and GOCE-TIM3 (lower panel) gravity models. The harmonic components from 90 to 120 (left), from 120 to 150 (middle) and from 150 to 180 (right) are shown. Units are cm s^{-1}.

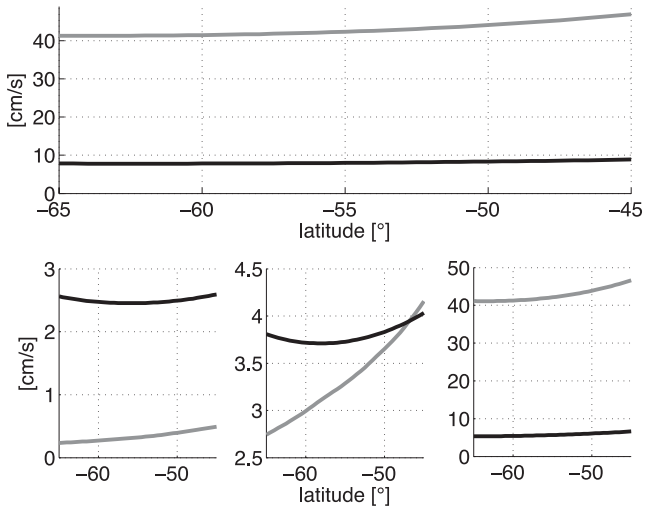

Figure 7. Comparison between the propagated errors from the harmonic coefficients to the geostrophic velocities in the ACC area as function of latitude. Two gravity models are considered: ITG-Grace2010 (grey line) and GOCE-TIM3 (black line). The error of the MSS is considered uncorrelated with an rms value equal to 3 cm. The upper panel shows the cumulative error up degree $L = 180$. In the lower panel the MDT errors in different bands are shown considering the harmonic components from 90 to 120 (left-hand panel), from 120 to 150 (middle panel) and from 150 to 180 (right-hand panel). Units are cm s^{-1}.

around the world, (Lumpkin & Pazos 2007). Each drifter location is estimated from 16 to 20 satellite fixes per day. These raw data are processed applying quality control procedures and interpolated via kriging to regular 6-hr intervals.

A large set of these data has been considered for our comparison, taking all the measurements from 1993 January to 2010 December, in the ACC area: latitude from 40S to 90S and longitude from 180E to 180W. In Grodsky *et al.* (2011) a problem in the Southern Ocean is discussed related to the more recent buoy models. Artificial accelerations have been observed after three months of measurements. For this reason, only the first 90 d of drifter data after 2004 January 1 are considered.

The drifter observations include tide currents, Ekman currents, inertial currents and high-frequency ageostrophic currents. In order to perform a correct comparison with the geostrophic velocities derived from the MDT, the drifter data must be corrected, in an attempt to extract only their geostrophic component. The Global Drifter Program provides a global estimate of the mean Ekman currents (Lumpkin & Garraffo 2005), derived using wind stress data and the local Coriolis parameter, (Ralph & Niiler 1999). This data set can be used to estimate the order of magnitude of the Ekman corrections, even if these averaged values refer to a period (from 1997 September 1997 to 2003 August) different from the period considered in the MSS DGFI10 computation. A second correction is to subtract the altimetric velocity anomaly corresponding to the Sea Level Anomalies (SLA). This is the so called synthetic method, see Rio *et al.* (2006). The global SLA are interpolated to a $30' \times 30'$

Table 2. Statistics of the differences between the geostrophic velocities of either GOCE or GRACE MDTs and the geostrophic velocities as derived from drifter data in the ACC area. In parenthesis the statistics relative to the region of the Drake Passage ($\varphi \in [-40^\circ, -60^\circ], \lambda \in [290^\circ, 320^\circ]$). Different resolutions are considered. Units are cm s^{-1}.

	Mean(Δv_s)	rms(Δv_s)	Mean(Δu_s)	rms(Δu_s)
GOCE MDT				
$L = 120$	4.18 (3.36)	5.24 (4.05)	−5.17 (−1.84)	7.17 (3.91)
$L = 150$	4.20 (3.38)	5.55 (4.49)	−5.19 (−1.88)	7.51 (4.63)
$L = 180$	4.20 (3.40)	6.34 (5.48)	−5.21 (−1.91)	8.12 (5.89)
GRACE MDT				
$L = 120$	4.17 (3.35)	5.37 (4.33)	−5.15 (−1.81)	7.27 (4.20)
$L = 150$	4.18 (3.36)	6.84 (6.93)	−5.17 (−1.90)	8.68 (7.30)
$L = 180$	4.17 (3.36)	10.36 (12.02)	−5.17 (−2.00)	7.27 (13.99)

grid every month from January 1993 to December 2010. For each grid point the corresponding geostrophic velocities are computed, through a simple numerical differentiation between adjacent grid points. Then each drifter measurement is corrected by subtracting the values of the SLA velocity of the corresponding month. Finally, the drifter data are gridded on a $30' \times 30'$ grid and spatially Gauss filtered with half-weight radius r consistent with the harmonic degree L of the spectral filter in eq. (5).

Statistics of the differences are summarized in Table 2. The mean of the differences is always different from zero, showing an offset (negative for the eastward component u_s and positive for the northward one v_s). Results considering GRACE MDT are comparable with GOCE MDT only up to $L = 120$. As resolution increases, GOCE is able to reproduce the currents better, even if the rms is not small, when compared with the rms of the signal [rms(u_s) = 15.57 cm s^{-1} and rms(v_s) = 10.73 cm s^{-1}]. If only the sub-region of the Drake Passage area is considered, the rms for both the components has an acceptable size, showing that strong regional variations exist. In this comparison, it should be noted that (i) the spatial distribution of the *in situ* measurements is by far not uniform and (ii) that the Ekman correction is an estimate not really temporally consistent with the MSS.

6 CONCLUSION

A geodetic MDT is determined from joint cross-over adjustment of 17 yr of multimission altimeter data and a recent gravity model from the GOCE mission. The proper representation of MDT is needed in order to describe the mean ocean geostrophic surface flow. One of the areas where this has been a challenge is Southern Ocean. Due to the strong winds that drive the ACC, presence of sea ice and strong variability, the Southern Ocean has not been well observed neither with satellite nor *in situ* measurements. The sparsity of *in situ* observations (in space and time) as well as complex topography still poses a challenge also for validation of the MDT products in Southern Ocean.

The MDT computed using only satellite data, from GOCE and altimetry, is of increased accuracy and resolution compared to GRACE and altimetry solution. The GOCE data are adding short wavelength geoid information, in particular above spherical harmonic degree 120, corresponding to spatial scales below 160 km. In this paper, we also described a technique of minimizing adverse effects of extension of MSS over the areas not covered by altimetric measurements. However, coastal zones remain the weak spot of the filtering process when following the spectral approach described here. Unfortunately, these zones are also problematic in terms of MSS calculations and ocean tide modelling.

From the MDT surface, velocities of comparable resolution are derived and analysed in spectral bands similarly to MDT. In this case the strength of GOCE at shorter scales is more pronounced since the geostrophic velocities are computed from gradients of MDT, amplifying the short scales proportionally to the spherical harmonic degree. The ACC currents based on GOCE seem now well defined and in good agreement with Subantarctic and Polar fronts estimated from *in situ* data. The agreement of the geostrophic velocities as derived from the geodetic MDT with those based on drifter data is acceptable, but it can be improved. The procedure for isolating the geostrophic part of drifter velocities (including realistic error estimates) can be refined. The spectral representation of MDT allows us to provide also estimates of uncertainty of the new MDT as well as of the geostrophic velocities. The values of which have strongly decreased from for GRACE only models to GOCE results. The improvement on the shorter scales involves a reduction of 75 per cent of the total error.

Further progress is expected from up-coming gravity models which will utilize a more extended ensemble of GOCE measurements and will be combined with GRACE information.

ACKNOWLEDGMENTS

This work has been funded under DFG Priority Research Programme SPP 1257 ‘Mass Transport and Mass Distribution in the Earth System’. The data and the products described in the paper can be requested from the authors. Sincere thanks go to the four anonymous reviewers who helped improve the paper.

REFERENCES

Albertella, A. & Rummel, R., 2009. On the spectral consistency of the altimetric ocean and geoid surface: a one-dimensional example, *J. Geod.,* **83,** 805–815, doi: 10.1007/s00190-008-0299-5.

Albertella, A., Wang, X. & Rummel, R., 2010. Filtering of altimetric sea surface heights with a global approach, in *Gravity, Geoid and Earth Observation*, IAG Symposia Vol. 135, pp. 247–252, ed. Mertikas, S.P., Springer, Berlin.

Andersen, O.B. & Knudsen, P., 2009. DNSC08 mean sea surface and mean dynamic topography models, *J. geophys. Res.,* **114,** C11001, doi:10.1029/2008JC005179.

Bingham, R.J., Haines, K. & Hughes, C.W., 2008. Calculating the ocean’s mean dynamic topography from a mean sea surface and a geoid, *J. Atmos. Ocean Technol.,* **25,** 1808–1822, doi:10.1175/2008JTECHO568.1.

Bingham, R.J., 2010. Nonlinear anisotropic diffusive filtering applied to the ocean’s mean dynamic topography, *Remote Sens. Lett.,* **1**(4), 205–212, doi:11.1080/01431161003743165.

Bingham, R.J., Knudsen, P., Andersen, O. & Pail, R., 2011. An initial estimate of the North Atlantic steady-state geostrophic circulation from GOCE, *Geophys. Res. Lett.,* **38,** 1, L01606, doi:10.1029/2010GL045633.

Chambers, D.P., Hayes, S.A., Ries, J.C. & Urban, T.J., 2003. New TOPEX sea state bias models and their effect on global mean sea level, *J. geophys. Res.,* **108**(C10), 3305, doi: 10.1029/2003JC001839.

Dettmering, D. & Bosch, W., 2010a. Global calibration of jason-2 by multimission crossover analysis, *Mar. Geod.,* **33**(S1), 150–161.

Dettmering, D. & Bosch, W., 2010b. Envisat radar altimeter calibration by multi-mission crossover analysis, in *Proceedings of the ESA Living Planet Symposium,* Bergen, Norway, ESA Publication SP-686 (CD-Rom).

Drinkwater, M.R., Floberghagen, R., Haagmans, R., Muzi, D. & Popescu, A., 2003. GOCE: ESA’s first Earth Explorer Core mission, in *Earth Gravity Field From Space—From Sensors to Earth Science,* Space Sci. Ser. ISSI, Vol. 18, pp. 419–432, eds Beutler, G. *et al.*, Kluwer Academic, Dordrecht.

Elema, I.A., 1993. Influence of geoid model uncertainty on the determination of the ocean circulation with satellite altimetry, *thesis*, Technische Universiteit Delft, faculteit der geodesie.

European Space Agency (ESA), 1998. *The science and research elements of ESA's living planet programme,* ESA SP-1227, European Space Agency, Noordwijk.

European Space Agency (ESA), 2006. *The changing earth,* ESA SP-1304, European Space Agency, Noordwijk.

Farrell, S.L., McAdoo, D., Laxon, S.W., Zwally, H.J., Yi, D., Ridout, A. & Giles, K., 2012. Mean dynamic topography of the Arctic Ocean, *Geophys. Res. Lett.,* **39,** L01601, doi:10.1029/2011GL050052.

Griesel, A., Mazloff, M.R. & Gille, S.T., 2012. Mean dynamic topography in the Southern Ocean: Evaluation Antartic Circumpolar Current transport, *J. geophys. Res.,* **117,** C01020, doi:10.1029/2011JC007573.

Grodsky, S.A., Lumpkin, R. & Carton, J.A., 2011. Spurious trends in global surface drifter currents, *Geophys. Res. Lett.,* **38,** L10606, doi:10.1029/2011GL047393.

Haines, K., Johannessen, J.A., Knudsen, P., Lea, D., Rio, M.H., Bertino, L., Davidson, F. & Hernandez, F., 2011. An ocean modelling and assimilation guide to using GOCE geoid products, *Ocean Sci.,* **7,** 151–164, doi:10.5194/os-7-151-2011.

Heiskanen, W.A. & Moritz, H., 1967. *Physical Geodesy,* Freeman, San Francisco, CA.

Hernandez, F. & Schaeffer, P., 2000. Altimetric mean sea surfaces and gravity anomaly maps inter-comparisons, CLS, AVI-NT-011-5242-CLS.

Hughes, C.W. & Bingham, J.R., 2008. An oceanographer's guide to GOCE and the geoid, *Ocean Sci. Discuss.,* **4,** 15–29.

Knudsen, P., Bingham, R., Andersen, O. & Rio, M.H., 2011. A global mean dynamic topography and ocean circulation estimation using a preliminary GOCE gravity model, *J. Geod.,* **85**(11), 861–879, doi:10.1007/s00190-011-0485-8.

Iijima, B.A. *et al.*, 1999. Automated daily process for global ionospheric total electron content maps and satellite ocean ionospheric calibration based on Global Positioning System, *J. Atmos. Solar-Terrest. Phys.,* **61,** 1205–1218.

Jekeli, C., 1981. Alternative methods to smooth the earth's gravity field, Rep.327, D. Sci. & Surv., Ohio State University, Columbus, OH.

Losch, M., Sloyan, B.M., Schröter, J. & Sneeuw, N., 2002. Box inverse models, altimetry and the geoid: problems with the omission error, *J. geophys. Res.,* **107**(C7), 3078, doi:10.1029/2001JC000855.

Lumpkin, R. & Garraffo, Z., 2005. Evaluating the decomposition of tropical Atlantic drifter observations, *J. Atmos. Oceanic Technol.,* **I22**(3078), 1403–1415.

Lumpkin, R. & Pazos, M., 2007. Measuring surface currents with surface velocity program drifters: the instrument, its data, and some recent results, in *Lagrangian Analysis and Prediction of Coastal and Ocean Dynamics (LAPCOD),* chapter 2, pp. 39–67, eds Griffa, A., Kirwan, A.D., Mariano, A.J., Ozgokmen, T. Rossby, T., Cambridge University Press, Cambridge.

Mayer-Gürr, T., Eicker, A., Kurtenbach, E. & Ilk, K.H., 2010. ITGGRACE: global static and temporal gravity field models from GRACE data, in *System Earth via Geodetic—Geophysical Space Techniques,* pp. 159–168, eds Flechtner, F. *et al.*, Springer, Berlin, doi:10.1007/978-3-642-10228-813.

Mayer-Gürr, T., Savcenko, R., Bosch, W., Daras, I., Flechtner, F. & Dahle, Ch., 2011 (online first). Ocean tides from satellite altimetry and GRACE, *J. Geodyn.,* in press, doi:10.1016/j.jog.2011.10.009.

Orsi, A.H., Whitworth, T., III, & Nowlin, W.D., Jr, 1995. On the meridional extent and fronts of the Antarctic circumpolar current, *Deep-Sea Res.,* **42,** 641–673.

Pail, R., Goiginger, H., Mayrhofer, R., Schuh, W.D., Brockmann, J.M., Krasbutter, I., Höck, E. & Fecher, T., 2010. Global gravity field model derived from orbit and gradiometry data applying the time-wise method, in *Proceedings of the ESA Living Planet Symposium,* Bergen, Norway, ESA Publication SP-686 (CD-Rom).

Pail, R. *et al.*, 2011. First GOCE gravity field models derived by three different approaches, *J. Geod.,* **85**(11), 819–843, ISSN:0949-7714, doi:10.1007/s00190-011-0467-x.

Ralph, E.A. & Niiler, P.P., 1999. Wind-driven currents in the Tropical Pacific, *J. Phys. Oceanogr.,* **29,** 2121–2129.

Rapp, R.H., 1989. The treatment of permanent tidal effects in the analysis of satellite altimeter data for sea surface topography, *Manuscripta Geodaetica,* **14**(6), 368–372.

Rio, M.-H., Schaeffer, P., Hernandez, F. & Lemoine, J.M., 2006. From the altimetric sea level measurement to the ocean absolute dynamic topography: Mean Sea Surface, Geoid, Mean Dynamic Topography, a three-component challenge, in *Proceedings of the 15 Years of Progress in Radar Altimetry Symposium,* Venice, Italy, 13–18 2006 March, ESA Special Publication SP-614.

Rummel, R., Balmino, G., Johannessen, J., Visser, P. & Woodworth, P., 2002. Dedicated gravity field missions—principles and aims, *J. Geodyn.,* **33**(1–2, 3–20), doi:10.1016/S0264-3707(01)00050-3.

Rummel, R. & Gruber, T., 2010. Gravity and steady-state ocean circulation explorer GOCE, in *System Earth via Geodetic—Geophysical Space Techniques,* pp. 203–212, eds Flechtner, F., Gruber, T., Güntner, A., Mandea, M., Rothacher, M., Schöne, T. & Wickert, J., Springer, Heidelberg.

Rummel, R., 2010. GOCE: gravitational gradiometry in a satellite, in *Handbook of Geo-Mathematics,* Part 2, pp. 93–103, Springer, Berlin, doi:10.1007/978-3-642-01546-5-4.

Scharroo, R. & Visser, P., 1998. Precise orbit determination and gravity field improvement for the ERS satellites, *J. geophys. Res.,* **103**(C4), 8113–8127.

Scharroo, R. & Smith, W.H.F., 2010. A global positioning system-based climatology for the total electron content in the ionosphere, *J. geophys. Res.,* **115,** A10318, doi:10.1029/2009JA014719.

Schrama, E., Scharroo, R. & Naeije, M., 2000. Radar Altimeter Database System (RADS): towards a generic multi-satellite altimeter database system, USP-2 report 00-11, BCRS/SRON, Delft.

Smith, D.A., 1998. There is no such thing as "The" EGM96 geoid: subtle points on the use of a global geopotential model, *IGeS Bull.,* **8,** 17–28.

Tapley, B.D., Chambers, D.P., Bettadpur, S. & Ries, J.C., 2003. Large scale ocean circulation from the GRACE GGM01 geoid, *Geophys. Res. Lett.,* **30,** 2163, doi:10.1029/2003GL018622.

Wahr, J., Molenaar, M. & Bryan, F., 1998. Time variability of the Earth's gravity field: hydrological and oceanic effects and their possible detection using GRACE, *J. geophys. Res.,* **103,** 30 205–30 229.

van Gelderen, M. & Koop, K., 1996. The use of degree variances in satellite gradiometry, *J. Geod.,* **71,** 337–343.

Zenner, L., 2006. Zeitliche Schwerefeldvariationen aus GRACE und Hydrologiemodellen, Diplomarbeit, TU München.